Harmonically-related diffraction gratings-based interferometer for quadrature phase measurements

Zahid Yaqoob, Jigang Wu, Xiquan Cui, Xin Heng, and Changhuei Yang

Department of Electrical Engineering, MC 136-93, California Institute of Technology, Pasadena, CA 91125
zyaqoob@caltech.edu

Abstract: We demonstrate the use of shallow diffraction gratings for quadrature phase interferometry. A single shallow diffraction grating-based Michelson interferometer yields only trivial (0^o or 180^o) phase shift between different output ports. In comparison, a combination of two parallel shallow diffraction gratings can be useful to achieve desired phase shifts (e.g., 90^o for quadrature phase interferometry). We show that the phase at different output ports of a grating-pair based interferometer can be adjusted by shearing the two gratings with respect to each other. Two harmonically-related diffraction gratings are used to demonstrate phase shift control at the output ports of a modified Michelson interferometer. Our experimental data is in good agreement with theory.

OCIS Codes: (120.2880) Holographic interferometry; (180.3170) Interference microscopy; (170.3880) Medical and Biological Imaging

References and links

1. J. C. Shaw, "Metrology using differential phase-contrast microscopy," Microelectron. Eng. **13**, 527-530 (1991).
2. P. J. McMahon, E. D. Barone-Nugent, B. E. Allman, and K. A. Nugent, "Quantitative phase-amplitude microscopy II: differential interference contrast imaging for biological TEM," J. Microsc.-Oxford **206**, 204-208 (2002).
3. F. Zernike, "Phase contrast, a new method for the microsopic observation of transparent objects," Physica **9**, 686-698 (1942).
4. F. Zernike, "Phase contrast, a new method for the microscopic observation of transparent objects Part II," Physica **9**, 974-986 (1942).
5. G. Nomarski, and A. R. Weill, "Application à la métallographie des méthodes interférentielles à deux ondes polarisées," Rev. Metall. **2**, 121-128 (1955).
6. W. Shimada, T. Sato, and T. Yatagai, "Optical surface microtopography using phase-shifting Nomarski microscope," Proc. SPIE **1332**, 525-529 (1990).
7. P. Hariharan, and M. Roy, "Achromatic phase-shifting for two-wavelength phase-stepping interferometry," Opt. Comm. **126**, 220-222 (1996).
8. C. J. Cogswell, N. I. Smith, K. G. Larkin, and P. Hariharan, "Quantitative DIC microscopy using a geometric phase shifter," Proc. SPIE **2984**, 72-81 (1997).
9. M. R. Arnison, C. J. Cogswell, N. I. Smith, P. W. Fekete, and K. G. Larkin, "Using the Hilbert transform for 3D visualization of differential interference contrast microscope images," J. of Microsc.-Oxford **199**, 79-84 (2000).
10. M. R. Arnison, K. G. Larkin, C. J. R. Sheppard, N. I. Smith, and C. J. Cogswell, "Linear phase imaging using differential interference contrast microscopy," J. of Microsc.-Oxford **214**, 7-12 (2004).
11. H. Ishiwata, M. Itoh, and T. Yatagai, "A new method of three-dimensional measurement by differential interference contrast microscope," Opt. Comm. **260**, 117-126 (2006).
12. U. Schnars, and W. Juptner, "Direct Recording of Holograms by a Ccd Target and Numerical Reconstruction," Appl. Opt. **33**, 179-181 (1994).
13. E. Cuche, F. Bevilacqua, and C. Depeursinge, "Digital holography for quantitative phase-contrast imaging," Opt. Lett. **24**, 291-293 (1999).
14. G. Popescu, T. Ikeda, C. A. Best, K. Badizadegan, R. R. Dasari, and M. S. Feld, "Erythrocyte structure and dynamics quantified by Hilbert phase microscopy," J. Biomed. Opt. **10**, (2005).
15. T. Ikeda, G. Popescu, R. R. Dasari, and M. S. Feld, "Hilbert phase microscopy for investigating fast dynamics in transparent systems," Opt. Lett. **30**, 1165-1167 (2005).

#72448 - $15.00 USD Received 28 June 2006; revised 15 August 2006; accepted 17 August 2006

16. D. S. Marx, and D. Psaltis, "Polarization quadrature measurement of subwavelength diffracting structures," Appl. Opt. **36**, 6434-6440 (1997).
17. D. O. Hogenboom, C. A. DiMarzio, T. J. Gaudette, A. J. Devaney, and S. C. Lindberg, "Three-dimensional images generated by quadrature interferometry," Opt. Lett. **23**, 783-785 (1998).
18. M. A. Choma, "Instantaneous quadrature low-coherence interferometry with 3 x 3 fiber-optic couplers," Opt. Lett. **28**, 2162 - 2164 (2003).
19. Z. Yaqoob, J. Fingler, X. Heng, and C. H. Yang, "Homodyne en face optical coherence tomography," Opt. Lett. **31**, 1815-1817 (2006).
20. B. L. Danielson, and C. Y. Boisrobert, "Absolute optical ranging using low coherence interferometry," Appl. Opt. **30**, 2975-2979 (1991).
21. V. V. Tuchin, "Coherence-domain methods in tissue and cell optics," Laser Phys. **8**, 807-849 (1998).
22. S. R. Thurber, A. M. Brodsky, and L. W. Burgess, "Characterization of random media by low-coherence interferometry," Appl. Spectrosc. **54**, 1506-1514 (2000).
23. D. Huang, E. A. Swanson, C. P. Lin, J. S. Schuman, W. G. Stinson, W. Chang, M. R. Hee, T. Flotte, K. Gregory, C. A. Puliafito, and J. G. Fujimoto, "Optical coherence tomography," Science **254**, 1178-1181 (1991).
24. C. M. B. Cordeiro, L. Cescato, A. A. Freschi, and L. F. Li, "Measurement of phase differences between the diffracted orders of deep relief gratings," Opt. Lett. **28**, 683-685 (2003).

1. Introduction

Highly accurate amplitude and phase measurements of optical signals are important in many applications ranging from metrology [1] to cell biology [2]. Traditional phase-contrast imaging techniques such as Zernike phase [3, 4] and Nomarski differential interference contrast (DIC) [5] render excellent phase contrast images; however, the phase information is only qualitative in nature. To retrieve quantitative phase information in Nomarski DIC, several approaches have been proposed that include: DIC with changing shear direction [6], phase shifting DIC [7, 8], and non-iterative phase reconstruction methods such as half-plane Hilbert transform [9]. In addition, Arnison et al. proposed a method that combined DIC microscopy with phase shifting, shear rotation, and Fourier phase integration to yield linear phase image of a sample [10]. Recently, Ishiwata et al. have developed retardation-modulated DIC - a method to extract the phase component from the DIC image using two images with different retardation [11].

Other methods for quantitative phase imaging (QPI) include digital holography [12, 13], Hilbert phase microscopy (HPM) [14, 15], and polarization based techniques [16, 17]. Interference microscopy techniques based on PSI generally require recording of four interferograms with precise $\pi/2$ phase shifts of the reference field, adding complexity to the system while others can be computation extensive. HPM and digital holography are simpler as they require only one interferogram for QPI. We note that the methods depend on recording of high frequency spatial fringes for successful phase unwrapping. We also note that multiport fiber based systems such as 3x3 couplers can provide non-trivial phase difference, which can be manipulated for quadrature phase measurements [18, 19]. However, free space equivalents of a 3x3 coupler do not exist.

In this letter, we report a new method for obtaining non-trivial phase difference between the output ports of a reflectance based interferometer through the use of shallow diffraction gratings. We show that as opposed to a single shallow diffraction grating-based interferometer (which provides only trivial phase shifts), a pair of harmonically-related shallow diffraction gratings can be used to realize a modified Michelson interferometer where the phase shifts between different output ports can be adjusted. More importantly, the phase shift can be adjusted by simply shearing one grating with respect to the other. This approach does not change the path length relationships of the different interference beams within the interferometer – an advantage for metrology [1] and low coherence interferometry applications [20-23].

This reported method to obtain non-trivial phase shift opens new possibilities for full-field quadrature phase interferometry.

#72448 - $15.00 USD Received 28 June 2006; revised 15 August 2006; accepted 17 August 2006

2. Phase of diffracted light in shallow gratings

The phase of transmitted / reflected and diffracted light in shallow diffraction gratings is a well understood quantity. However, for the sake of completeness, we provide a brief account of how a diffraction grating affects the phase of light. Consider a sinusoidal phase grating (see Fig. 1).

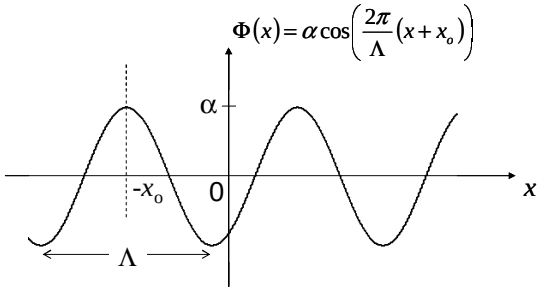

Fig. 1. Spatial phase modulation in a sinusoidal phase grating.

The complex transmittance of a sinusoidal phase grating can be expressed as:

$$t(x)=\exp\left\{j\alpha\cos\left(\frac{2\pi}{\Lambda}(x+x_o)\right)\right\}, \tag{1}$$

where α, Λ, and x_o are the amplitude of phase modulation, period, and displacement from the origin along *x*-direction, respectively, of the phase grating. Defining $\xi(x_o)=2\pi x_o/\Lambda$, we can rewrite Eq. (1) in the form:

$$t(x)=\sum_{m=-\infty}^{\infty}J_m(\alpha)\exp\left\{jm\left(\frac{2\pi}{\Lambda}x+\xi(x_o)+\frac{\pi}{2}\right)\right\}, \tag{2}$$

where $J_m(\alpha)$ is m^{th} order Bessel function of the first kind. Using the identity $J_{-m}(\alpha)=(-1)^m J_m(\alpha)$, the relative phase of the m^{th} diffracted order with respect to the zeroth order is given by:

$$\phi(x_o)=\begin{cases} m\left\{\xi(x_o)+\frac{\pi}{2}\right\}, & m\geq 1 \\ |m|\left\{-\xi(x_o)+\frac{\pi}{2}\right\}. & m\leq 1 \end{cases} \tag{3}$$

It should be noted that for shallow phase gratings, Eq. (3) holds regardless of the grating profile [24].

3. Single grating-based Michelson interferometer

Diffraction gratings can be used as beam splitters in different interferometric designs. As mentioned earlier, the diffracted light in diffraction gratings acquires a unique phase with respect to the undiffracted light. Moreover, this distinct phase $\phi(x_o)$ can be adjusted by translating the diffraction grating in *x*-direction [see Eq. (3)]. However, the phase shifts between different output ports of single grating-based Michelson / Mach-Zehnder interferometers are only trivial in nature. To better understand this phenomenon and the operation of our harmonically-related gratings-based interferometer, we start by examining a simpler system – a Michelson interferometer based on a single shallow diffraction grating G_1 [see Fig. 2(a), and 2(b)].

#72448 - $15.00 USD Received 28 June 2006; revised 15 August 2006; accepted 17 August 2006

In the arrangement shown in Fig. 2(a), a collimated beam from a laser source is directed at normal incidence at G_1, which acts as a beam splitter during the first diffraction. Only two beams are considered, i.e., the zeroth order (black line) and a first order diffracted beam (red line) which form the sample and reference arms, respectively, of the Michelson interferometer. Note that the grating period Λ_1 can be chosen so that only the zeroth and the first order diffracted beams exist. Mirror M_1 is shown as the sample whereas M_2 represents the reference mirror. The returning sample and reference beams reach the grating G_1 and undergo a second diffraction. At this time, the grating acts both as a beam splitter as well as a combiner, since it splits and combines the incoming sample and reference beams at the three output ports I, II, and III of the interferometer. The coincident reference and sample beams at the three ports are shown as dashed black and red lines [see Fig. 2(b)]. A beam splitter (BS) is used to separate the output beam at port II from the input beam. In the context of Figs. 2(c)-2(e), which illustrate the phase of the diffracted beams with respect to the undiffracted beams during the two passes, the total electric field at port I of the single grating-based interferometer can be written as:

$$\begin{aligned} E_I &= E_1 \exp\{i(2kd_1 - \xi_1(x_1) + \pi/2)\} \quad \rightarrow \text{ Field comp. from the sample arm} \\ &\quad + E_2 \exp\{i(2kd_2 + \xi_1(x_1) + \pi/2)\}, \quad \rightarrow \text{ Field comp. from the reference arm} \end{aligned} \tag{4}$$

where E_1 and E_2 are the amplitudes of the field components reaching port I from the sample and reference arms, respectively. k is the optical wave vector, and the parameters d_1 and d_2 correspond to the path lengths of the sample and reference arms, respectively. Moreover, $\xi_1(x_1) = 2\pi x_1 / \Lambda_1$, where x_1 is the displacement of the grating G_1. Therefore, using $E_I E_I^*$, the interference signal at port I of the interferometer can be written as:

$$i_I = 2A_1 \cos\{2k(d_2 - d_1) + 2\xi_1(x_1)\}, \tag{5a}$$

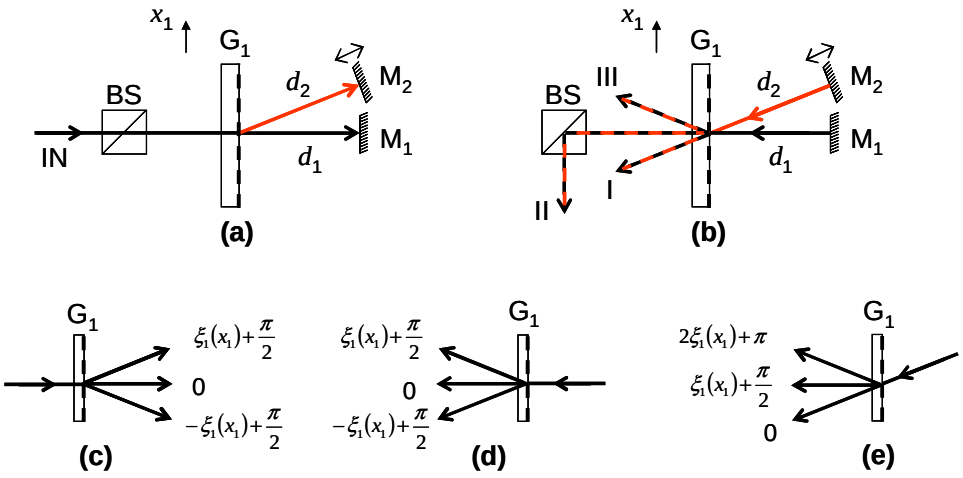

Fig. 2. (a, b) Schematic of a Michelson interferometer using a single shallow diffraction grating, G_1. (a) The transmitted sample beam and the diffracted reference beam are shown in black and red solid lines, respectively. (b) shows dashed black and red lines representative of coincident sample and reference beam at output ports I, II, and III of the interferometer. (c) Phase shift of the diffracted beam with respect to the undiffracted beam during the first diffraction. (d,e) Phase shifts of the diffracted sample and reference beams, respectively, during the second diffraction. x_1 is the actuation of grating G_1 along the x-direction for the experiment, whereas d_1 and d_2 represent path lengths of sample and reference arms, respectively. M_i: ith Mirror; BS: Beam splitter.

Similarly, the interference signals at ports II and III of the interferometer can be written as:

#72448 - $15.00 USD Received 28 June 2006; revised 15 August 2006; accepted 17 August 2006

$$i_{II} = 2A_2 \cos\{2k(d_2 - d_1) + 2\xi_1(x_1) + \pi\}, \quad (5b)$$

$$i_{III} = 2A_3 \cos\{2k(d_2 - d_1) + 2\xi_1(x_1) + \pi\}, \quad (5c)$$

respectively. The parameters A_i, i = 1, 2, 3 are the amplitudes of the interference signals at ports I, II, and III, respectively, and depend upon the diffraction efficiency of the grating G_1. It is clear from Eq. (5) that ports II and III of a single shallow grating-based Michelson interferometer are in phase whereas the port I of the interferometer is 180° out of phase with respect to the other two output ports. This geometry is therefore unsuitable for extracting quadrature signals.

To corroborate the above discussion, an experimental setup was made using a collimated beam ($1/e^2$ diameter ≈ 1 mm) from a HeNe laser (λ = 633 nm) and a shallow 600 grooves/mm blazed transmission grating (Thorlabs, Inc., GT25-06V). The reference mirror was mounted on a voice coil to modulate the reference arm. Heterodyne interference signals were acquired at the three output ports using New Focus photodetectors (model 2001) and a 16-bit analog-to-digital converter (National Instruments, model PXI-6120). The grating was mounted on a computer-controlled piezo actuator (25.5 nm/V) in order to measure the phase shifts between different ports of the interferometer for various positions of the grating. For each position of the grating, DC components were removed from the acquired heterodyne signals at the three ports; the resulting interference signals, represented by Eqs. (5a)-(5c), were subsequently processed to determine the phase shifts between the output ports. Figure 3 shows the measured phase shifts between different output ports of the interferometer versus grating displacement over 3.5 microns (~ 2 grating periods) along the x_1 direction specified in Figs. 2(a),and 2(b). As expected, ports II and III are in phase whereas port I is ~180° out of phase with respect to the ports II and III, indicating that a single shallow diffraction grating-based Michelson interferometer cannot provide but trivial phase shifts between different output ports. Although, *p*-polarized light was used in this reported experiment (see results in Fig. 3), similar results were observed for the *s*-polarized light.

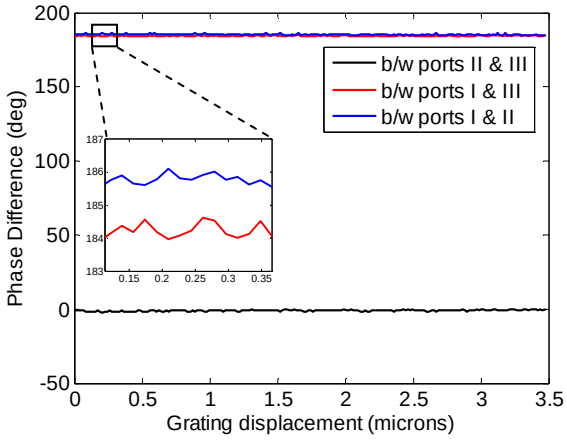

Fig. 3. Measured phase shifts between different ports of a single grating-based Michelson interferometer versus grating displacement (x_1) along the *x*-direction.

4. Harmonically-related grating pair-based Michelson interferometer

As illustrated by Eq. (5a)-Eq. (5c), a non-trivial phase shift given by $2\xi_1(x_1)$ is conferred on the interference term associated with each output port of a single-grating based interferometer. Since the amount of non-trivial phase shift is the same for each output port, the configuration shown in Figs. 2(a) and 2(b) yields only trivial phase difference between the output ports. This illustrates that it is not possible for a single shallow grating based interferometer, the

#72448 - $15.00 USD Received 28 June 2006; revised 15 August 2006; accepted 17 August 2006

Michelson interferometer described above or the Mach Zehnder configuration described in Ref. [24], to operate as a quadrature phase interferometer.

Fortunately, this effect does not extend to interferometers that contain two or more shallow gratings. In this section, we report on a modified Michelson interferometer based on two harmonically-related shallow diffraction gratings [see Figs. 4(a) and 4(b)] that can be adjusted to form a quadrature phase interferometer.

We choose the period of first grating G_1 as twice the period of the second grating G_2. The two gratings are placed at distance d_1 and aligned such that the grating planes as well as grating vectors are parallel to that of each other. Two mirrors M_1 and M_2 are introduced in the setup and aligned such that the first order diffracted beams (solid green and red lines) from G_1 meet with the undiffracted beam (solid black line) at G_2 [see Fig. 4(a)]. Moreover, the angle of incidence for the two beams at G_2 is the same as the angle of diffraction θ at G_1.

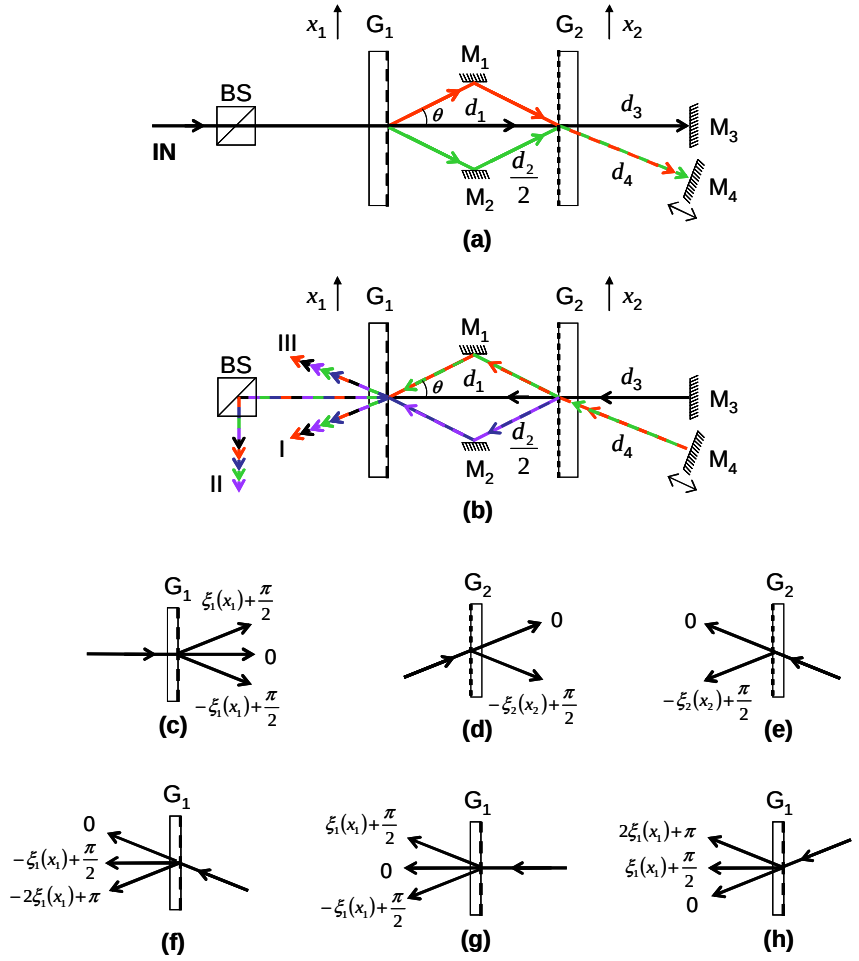

Fig. 4. (a, b). Modified Michelson interferometer design based on two harmonically-related shallow transmission gratings, where d_1 is the inter-grating distance and θ is the angle of diffraction. The sample and reference beams are shown as solid black and dashed red-green lines, respectively. (c)-(h) Phase shifts of the diffracted and undiffracted light during the first and second diffractions at gratings G_1 and G_2. Parameters x_1 and x_2 correspond to the actuations of grating G_1 and G_2, respectively, whereas d_3 and d_4 represent the path lengths of the sample and reference arms, respectively. M_i: ith Mirror; BS: Beam splitter.

For a given inter-grating distance d_1, the two first order diffracted beams will travel the same distance $d_2 = d_1/\cos(\theta)$ between G_1 and G_2. The grating G_2 combines the two first order

#72448 - $15.00 USD Received 28 June 2006; revised 15 August 2006; accepted 17 August 2006

beams from G_1 to form the reference beam (dashed red-green line) as shown in Fig. 4(a). The undiffracted beam from G_1 passes straight through G_2 to form the sample arm of the interferometer.

We note that fine alignment between the grating vectors is important in the proposed scheme for non–trivial phase shifts. The grating vectors alignment can be ensured by observing the interference pattern of reference beam arriving at mirror M_4. As mentioned earlier, the reference beam (represented by dashed red-green line) is comprised of two field components. Without proper alignment of the grating vectors, the interference of the two field components will form fringes at mirror M_4. However, by adjusting the grating vector alignment of the grating G_2, the fringes can be transformed into a bull's eye pattern – a representative of exact alignment of the grating vectors.

The returning sample beam arrives straight at G_1 whereas the reference arm beam reaches G_1 through the two possible paths set by the grating G_2 and mirrors M_1 and M_2. The portion of returning reference beam that passes through G_2 undiffracted is shown as dashed red-green line whereas the diffracted component is represented by dashed purple-blue line [see Fig. 4(b)]. Next, the grating G_1 splits and combines the incoming sample and reference beams at ports I, II, and III of the interferometer; the coincident five field components are represented by a five-colored dashed line at each output port. Figures 4(c)-4(h) show the phase of different beams as they undergo diffraction at G_1 and G_2 during their trip from the input port to the output ports of the modified Michelson interferometer. The total electric field at port I of the harmonically-related grating pair based interferometer can be written as:

$$
\begin{aligned}
E_{\mathrm{I}} = \exp\{i2k(d_2 + d_4)\} \qquad & (6)\\
\times \big[E_{\mathrm{I},1} \exp\{i(\xi_1(x_1) + \pi/2)\} \qquad & \rightarrow \text{Field comp. from ref. arm via } M_1, M_4, M_1\\
+ E_{\mathrm{I},2} \exp\{i(-\xi_1(x_1) - \xi_2(x_2) + 2\pi)\} \qquad & \rightarrow \text{Field comp. from ref. arm via } M_1, M_4, M_2\\
+ E_{\mathrm{I},3} \exp\{i(-\xi_1(x_1) - \xi_2(x_2) + \pi)\} \qquad & \rightarrow \text{Field comp. from ref. arm via } M_2, M_4, M_1\\
+ E_{\mathrm{I},4} \exp\{i(-3\xi_1(x_1) - 2\xi_2(x_2) + \pi/2)\}\big] \qquad & \rightarrow \text{Field comp. from ref. arm via } M_2, M_4, M_2\\
+ E_{\mathrm{I},5} \exp\{i2k(d_1 + d_3)\}\exp\{i(-\xi_1(x_1) + \pi/2)\}. \qquad & \rightarrow \text{Field comp. from the sample arm}
\end{aligned}
$$

In Eq. (6), the path lengths d_3 and d_4 are related to the sample and reference arms, respectively. The parameters $E_{\mathrm{I},1}$ to $E_{\mathrm{I},4}$ are the amplitudes of field components from the reference arm whereas $E_{\mathrm{I},5}$ is the amplitude of the field component from the sample arm arriving at port I of the interferometer. Furthermore, $\xi_1(x_1) = 2\pi x_1 / \Lambda_1$ (as defined earlier) and $\xi_2(x_2) = 2\pi x_2 / \Lambda_2$. The parameters x_2 and Λ_2 are the displacement and period, respectively, of the second grating G_2.

As labeled in Eq. (6), the first four terms represent the field components arriving at the output port I from the reference arm. This is because there are two possible paths (via mirrors M_1 and M_2) to transit between gratings G_1 and G_2. The 5th term in Eq. (6) is the field component contributed by the sample arm. We also note that by shearing the grating G_2 with respect to G_1, the phase of 2nd to 4th reference field components can be adjusted. As a note, if either of the paths (via mirrors M_1 and M_2) were blocked, only 1st or 4th term will remain (as contribution from the reference arm) that will yield trivial phase shifts similar to that in a single grating-based interferometer design.

From Eq. (6), we can express the interference signal at the output port I of the interferometer [shown in Fig. 4(a), and 4(b)] can be written as:

$$
\begin{aligned}
i_{\mathrm{I}}(x_1, x_2) = 2E'(x_1, x_2)E_{\mathrm{I},5} \cos[2k(d_4 - d_3 + d_2 - d_1) + \\
\phi'(x_1, x_2) - 2\{\xi_2(x_2) + \xi_1(x_1)\}], \qquad (7a)
\end{aligned}
$$

where

#72448 - $15.00 USD Received 28 June 2006; revised 15 August 2006; accepted 17 August 2006

$$E'(x_1,x_2)=\sqrt{F_1^2(x_1,x_2)+F_2^2(x_1,x_2)}\,,\qquad \phi'(x_1,x_2)=\tan^{-1}\left[\frac{F_2(x_1,x_2)}{F_1(x_1,x_2)}\right] \tag{7b}$$

such that

$$F_1(x_1,x_2)=E_{\mathrm{I},1}\cos\{4\xi_1(x_1)+2\xi_2(x_2)\}+(E_{\mathrm{I},2}-E_{\mathrm{I},3})\sin\{2\xi_1(x_1)+\xi_2(x_2)\}+E_{\mathrm{I},4}\,, \tag{7c}$$

$$F_2(x_1,x_2)=E_{\mathrm{I},1}\sin\{4\xi_1(x_1)+2\xi_2(x_2)\}-(E_{\mathrm{I},2}+E_{\mathrm{I},3})\cos\{2\xi_1(x_1)+\xi_2(x_2)\}. \tag{7d}$$

The amplitudes of the field components can be written in terms of diffraction efficiencies of the gratings G_1 and G_2 as:

$$E_{\mathrm{I},1}=\sqrt{\eta_{1,24}\eta_{2,43}\eta_{2,34}\eta_{1,43}}\,, \tag{8a}$$

$$E_{\mathrm{I},2}=\sqrt{\eta_{1,24}\eta_{2,43}\eta_{2,36}\eta_{1,63}}\,, \tag{8b}$$

$$E_{\mathrm{I},3}=\sqrt{\eta_{1,26}\eta_{2,63}\eta_{2,34}\eta_{1,43}}\,, \tag{8c}$$

$$E_{\mathrm{I},4}=\sqrt{\eta_{1,26}\eta_{2,63}\eta_{2,36}\eta_{1,63}}\,, \tag{8d}$$

$$E_{\mathrm{I},5}=\sqrt{\eta_{1,25}\eta_{2,52}\eta_{2,25}\eta_{1,53}}\,, \tag{8e}$$

where $\eta_{i,mn}$ is the diffraction efficiency of *i*th grating from port *m* to *n* (see Fig. 5 that labels different ports of the gratings G_1 and G_2).

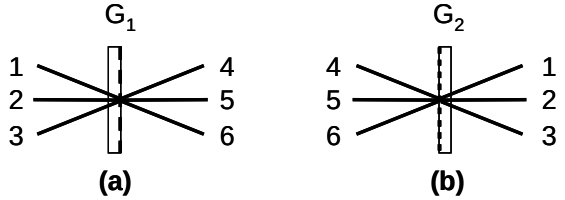

Fig. 5. Schematics labeling different ports of gratings G_1 and G_2.

Similarly, the interference signal at port II of the interferometer can be expressed as:

$$i_{\mathrm{II}}(x_1,x_2)=2E''(x_1,x_2)E_{\mathrm{II},5}\cos[2k(d_4-d_3+d_2-d_1)+\phi''(x_1,x_2)-2\{\xi_2(x_2)+\xi_1(x_1)\}], \tag{9a}$$

where

$$E''(x_1,x_2)=\sqrt{F_3^2(x_1,x_2)+F_4^2(x_1,x_2)}\,,\qquad \phi''(x_1,x_2)=\tan^{-1}\left[\frac{F_4(x_1,x_2)}{F_3(x_1,x_2)}\right] \tag{9b}$$

such that

$$F_3(x_1,x_2)=-E_{\mathrm{II},1}\cos\{4\xi_1(x_1)+2\xi_2(x_2)\}+(E_{\mathrm{II},2}+E_{\mathrm{II},3})\sin\{2\xi_1(x_1)+\xi_2(x_2)\}+E_{\mathrm{II},4}\,, \tag{9c}$$

$$F_4(x_1,x_2)=-E_{\mathrm{II},1}\sin\{4\xi_1(x_1)+2\xi_2(x_2)\}-(E_{\mathrm{II},2}+E_{\mathrm{II},3})\cos\{2\xi_1(x_1)+\xi_2(x_2)\}. \tag{9d}$$

In Eqs. (9a)-(9d), $E_{\mathrm{II},1}$ to $E_{\mathrm{II},4}$ represent the amplitudes of field components from the reference arm whereas $E_{\mathrm{II},5}$ is the amplitude of the field component from the sample arm arriving at port

#72448 - $15.00 USD Received 28 June 2006; revised 15 August 2006; accepted 17 August 2006

II of the interferometer, which are given in terms of diffraction efficiencies of the gratings G_1 and G_2 as:

$$E_{\mathrm{II},1} = \sqrt{\eta_{1,24}\eta_{2,43}\eta_{2,34}\eta_{1,42}}\,, \tag{10a}$$

$$E_{\mathrm{II},2} = \sqrt{\eta_{1,24}\eta_{2,43}\eta_{2,36}\eta_{1,62}}\,, \tag{10b}$$

$$E_{\mathrm{II},3} = \sqrt{\eta_{1,26}\eta_{2,63}\eta_{2,34}\eta_{1,42}}\,, \tag{10c}$$

$$E_{\mathrm{II},4} = \sqrt{\eta_{1,26}\eta_{2,63}\eta_{2,36}\eta_{1,62}}\,, \tag{10d}$$

$$E_{\mathrm{II},5} = \sqrt{\eta_{1,25}\eta_{2,52}\eta_{2,25}\eta_{1,52}}\,. \tag{10e}$$

In a similar fashion, the interference signal at port III of the interferometer is written as:

$$i_{\mathrm{III}}(x_1,x_2) = 2E'''(x_1,x_2)E_{\mathrm{III},5}\cos[2k(d_4-d_3+d_2-d_1)+ \phi'''(x_1,x_2)-2\{\xi_2(x_2)+\xi_1(x_1)\}+\pi], \tag{11a}$$

where

$$E'''(x_1,x_2) = \sqrt{F_5^2(x_1,x_2)+F_6^2(x_1,x_2)}, \qquad \phi'''(x_1,x_2) = \tan^{-1}\left[\frac{F_6(x_1,x_2)}{F_5(x_1,x_2)}\right] \tag{11b}$$

such that

$$F_5(x_1,x_2) = E_{\mathrm{III},1}\cos\{4\xi_1(x_1)+2\xi_2(x_2)\}+(E_{\mathrm{III},2}-E_{\mathrm{III},3})\sin\{2\xi_1(x_1)+\xi_2(x_2)\}+E_{\mathrm{III},4}\,, \tag{11c}$$

$$F_6(x_1,x_2) = E_{\mathrm{III},1}\sin\{4\xi_1(x_1)+2\xi_2(x_2)\}+(E_{\mathrm{III},3}-E_{\mathrm{III},2})\cos\{2\xi_1(x_1)+\xi_2(x_2)\}. \tag{11d}$$

In Eqs. (11a)-(11d), $E_{\mathrm{III},1}$ to $E_{\mathrm{III},4}$ correspond to the amplitudes of field components from the reference arm whereas $E_{\mathrm{III},5}$ denotes the amplitude of the field component from the sample arm arriving at port III of the interferometer. In terms of the diffraction efficiencies of the gratings G_1 and G_2, the amplitudes of above mentioned field components are given by:

$$E_{\mathrm{III},1} = \sqrt{\eta_{1,24}\eta_{2,43}\eta_{2,34}\eta_{1,41}}\,, \tag{12a}$$

$$E_{\mathrm{III},2} = \sqrt{\eta_{1,24}\eta_{2,43}\eta_{2,36}\eta_{1,61}}\,, \tag{12b}$$

$$E_{\mathrm{III},3} = \sqrt{\eta_{1,26}\eta_{2,63}\eta_{2,34}\eta_{1,41}}\,, \tag{12c}$$

$$E_{\mathrm{III},4} = \sqrt{\eta_{1,26}\eta_{2,63}\eta_{2,36}\eta_{1,61}}\,, \tag{12d}$$

$$E_{\mathrm{III},5} = \sqrt{\eta_{1,25}\eta_{2,52}\eta_{2,25}\eta_{1,51}}\,. \tag{12e}$$

It can be seen from Eqs. (7)-(12) that the amplitude and phase of the interference signals at the three ports I, II, and III not only depend on the strength of individual field components taking part in the interference but also on the additional phase shifts from gratings G_1 and G_2.

For clarity, we take a closer look at the interference signals, given by Eqs. (7a), (9a) and (11a), at the three output ports. It can be seen that the non-trivial phase term $2[\xi_2(x_2)+\xi_1(x_1)]$ is mutual to all the three interference terms. It, therefore, yields a trivial phase shift between different output ports. The non-trivial phase terms in Eqs. (7a), (9a) and (11a), which play a role in providing a non-trivial phase shift between the output ports, are $\phi'(x_1,x_2)$, $\phi''(x_1,x_2)$, and $\phi'''(x_1,x_2)$, respectively. These phase terms do not depend on the path lengths and can be solely adjusted by shearing of the harmonically-related gratings.

#72448 - $15.00 USD Received 28 June 2006; revised 15 August 2006; accepted 17 August 2006

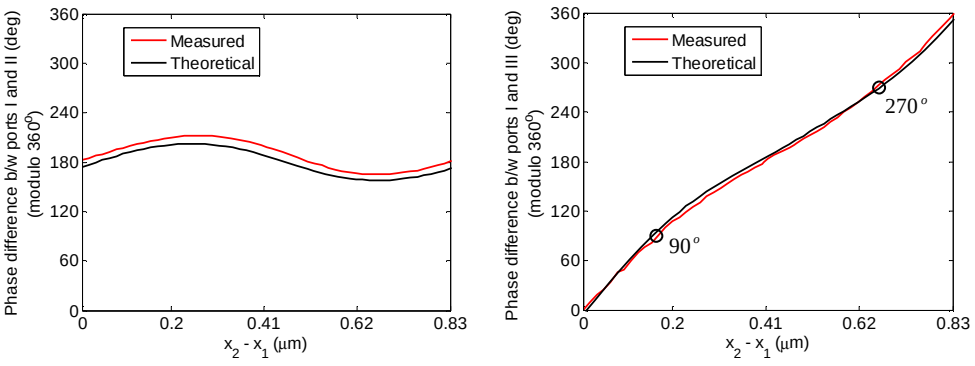

Fig. 6. Measured phase shifts between (a) ports I & II and (b) ports I & III of a harmonically-related gratings based modified Michelson interferometer versus shearing of grating G_2 with respect to G_1. The locations where phase difference between port I and III are equal 90° and 270° are labeled.

The only phase term that involves the path lengths d_i, i = 1, 2, 3, 4 is $2k(d_4 - d_3 + d_2 - d_1)$, and is common to all the three interference signals. As such, it yields only a trivial phase between different output ports. This also illustrates that in the described scheme, the shearing of the gratings to achieve non-trivial phase does not change the path length relationship between the interference beams at the output ports of the modified Michelson interferometer.

For experimental verification, we realized a setup shown in Figs. 4(a), and 4(b). A collimated beam ($1/e^2$ diameter ≈ 1 mm) from a 633 nm HeNe laser was used in the experiment. We chose G_1 to be the same as that used in the setup shown in Fig. 2(a) whereas G_2 – the second harmonic grating was selected as 1200 grooves/mm blazed transmission grating (Thorlabs, Inc., GT25-12). The path length d_1 between the gratings G_1 and G_2 was ~20 cm. The reference mirror M_4 was mounted on a voice coil to modulate the reference arm. The grating G_2 was translated along the *x*-direction using a piezo actuator (25.5 nm/V) and heterodyne interference signals were acquired at the three output ports using the same photodetectors as used in our earlier experimental study.

Table 1. Measured efficiencies of the gratings used in the setup shown in Figs. 4(a), and 4(b). These diffraction efficiencies were used to determine the theoretical phase shifts between different output ports of the modified Michelson interferometer.

600 grooves/mm				1200 grooves/mm			
$\eta_{1,14}$	0.001	$\eta_{1,41}$	0.001	$\eta_{2,14}$	0.12	$\eta_{2,41}$	0.11
$\eta_{1,15}$	0.43	$\eta_{1,51}$	0.43				
$\eta_{1,16}$	0.28	$\eta_{1,61}$	0.28	$\eta_{2,16}$	0.75	$\eta_{2,61}$	0.73
$\eta_{1,24}$	0.44	$\eta_{1,42}$	0.42				
$\eta_{1,25}$	0.23	$\eta_{1,52}$	0.24	$\eta_{2,25}$	0.67	$\eta_{2,52}$	0.67
$\eta_{1,26}$	0.11	$\eta_{1,62}$	0.11				
$\eta_{1,34}$	0.14	$\eta_{1,43}$	0.19	$\eta_{2,34}$	0.70	$\eta_{2,43}$	0.69
$\eta_{1,35}$	0.10	$\eta_{1,53}$	0.13				
$\eta_{1,36}$	0.05	$\eta_{1,63}$	0.06	$\eta_{2,36}$	0.10	$\eta_{2,63}$	0.11

$\eta_{i,mn}$: Diffraction efficiency of i^{th} grating from port *m* to port *n*.

#72448 - $15.00 USD Received 28 June 2006; revised 15 August 2006; accepted 17 August 2006

Figure 6 shows both the measured as well as the theoretical phase differences between output ports of the interferometer versus shearing of grating G_2 up to one grating periods. Table 1 shows measured diffraction efficiencies of gratings G_1 and G_2 (used in the setup) to calculate theoretical phase shifts between different ports of the interferometer. It can be seen that phase shift between ports I and III changes almost in a linear fashion as the grating G2 is sheared along the x_2 direction. This ability to achieve non-trivial phase shifts illustrates the possibility to design gratings-based interferometer for full-field quadrature phase interferometry.

This experiment does require gratings that are uniform and harmonically-related over the area of the incident beams. Based on the goodness-of-fit of our measurements, the gratings do appear to be well behaved over the area of our beams in the experiment.

5. Summary and conclusion

In summary, we have proposed and experimentally demonstrated the use of planar shallow diffraction gratings in a modified Michelson interferometric setup to achieve non-trivial phase shifts between different output ports. The phase shift is adjusted by simply shearing the gratings with respect to each other. The ability to adjust the phase shifts between different ports of the interferometer is a useful feature of the design for quadrature phase interferometry. The main advantage of the proposed method for non-trivial phase is that the shearing of the gratings does not change the path length relationship between interference beams at the output ports of the interferometer – an advantage for metrology and low coherence interferometry applications. Note that a single shallow diffraction grating-based Michelson interferometer cannot provide but trivial phase shifts between different output ports; hence, it is not suitable for quadrature phase measurements.

In a proof-of-concept experiment, we have used 600 grooves/mm and 1200 grooves/mm shallow diffraction gratings to demonstrate the phase shift control between various ports of the modified Michelson interferometer. The experimental data is in good agreement with the theoretical results calculated for our proposed harmonically-related gratings-based interferometer scheme. The initial study is promising and sets the stage for future progress in grating based quadrature phase imaging.

Another permutation for harmonically-related grating-based Michelson interferometer is to use the port 1 (instead of port 2) of the grating G_2 (see Fig. 5) to realize the sample arm. However, this new design will generate a total of eight field components (four from sample arm and another four from the reference arm) at each output port of the interferometer. Here, an interesting question arises as whether we can also use two similar gratings (e.g., a G_1G_1 combination as opposed the G_1G_2 combination) in the design shown in Fig. 4(a), and 4(b). As a matter of fact, it is possible to use two similar gratings to control phase shift between different output ports. However, this design will yield twelve field components (six each from the reference and sample arms) at each output port. The complexity of similar gratings-based interferometer design can be reduced if one of the mirrors, i.e., M_1 or M_2 is removed. This will reduce the total number of field components at each output port to eight. Nonetheless, the harmonically-related gratings-based modified Michelson interferometer proposed and demonstrated in this paper yields only a total of five field components at each output port and is, to our knowledge, the simplest gratings-based quadrature phase interferometric design.

An additional advantage of using harmonically-related gratings (as opposed to similar gratings) is that they can also be fabricated or holographically recorded on a single substrate, making it possible to design compact imaging systems for full-field quadrature interferometry. Finally, we believe that the concepts of harmonically-related gratings-based interferometer can be easily translated to X-rays as well, making it possible to realize X-ray systems for quadrature phase measurements.

Acknowledgment

The authors acknowledge helpful discussions with Demetri Psaltis and Marinko Sarunic. This work is supported by NSF career award BES-0547657.

#72448 - $15.00 USD Received 28 June 2006; revised 15 August 2006; accepted 17 August 2006